

Pyriproxyfen-based Rumino-Reticulum Device for horn fly control in cattle: development and characterization

Melina Cardilo Campos Alves¹ , Renata Nunes Oliveira³ , Gabriela Ferreira de Oliveira² ,
Thais Paes Ferreira² , Antonieta Middea⁴ , Maria Inês Bruno Tavares⁵ , Hugo Sabeça² ,
Bruno de Toledo Gomes¹ , Luiz Henrique Guerreiro Rosado⁶ , Fábio Barbour Scott² 
and Yara Peluso Cid^{6*} 

¹*Programa de Pós-graduação em Ciências Veterinárias, Laboratório de Quimioterapia Experimental em Parasitologia Veterinária – LQEPV, Instituto de Veterinária, Universidade Federal Rural do Rio de Janeiro – UFRRJ, Seropédica, RJ, Brasil*

²*Laboratório de Quimioterapia Experimental em Parasitologia Veterinária – LQEPV, Departamento de Parasitologia Animal, Instituto de Veterinária, Universidade Federal Rural do Rio de Janeiro – UFRRJ, Seropédica, RJ, Brasil*

³*Departamento de Engenharia Química, Instituto de Tecnologia, Universidade Federal Rural do Rio de Janeiro – UFRRJ, Seropédica, RJ, Brasil*

⁴*Setor de Caracterização Tecnológica, Centro de Tecnologia Mineral – CETEM, Universidade Federal do Rio de Janeiro – UFRJ, Rio de Janeiro, RJ, Brasil*

⁵*Instituto de Macromoléculas Professora Eloisa Mano, Universidade Federal do Rio de Janeiro – UFRJ, Rio de Janeiro, RJ, Brasil*

⁶*Departamento de Ciências Farmacêuticas, Instituto de Ciências Biológicas e da Saúde, Universidade Federal Rural do Rio de Janeiro – UFRRJ, Seropédica, RJ, Brasil*

*yarapcid@gmail.com

Abstract

This study aimed to develop a pyriproxyfen-based Rumino-Reticulum Device (RRD) consisting of films of poly(vinyl alcohol) (PVA) and sodium carboxymethylcellulose (NaCMC) to control the horn fly in cattle, one of the major pests of livestock. Films were obtained by the solvent casting method by PVA/NaCMC crosslinking and presented satisfactory homogeneity, drug content (104.8%) and pH (6.5), besides great absorptive capacity with swelling degree of 331.40% after 1 hour and diffusion-controlled release kinetics (Higuchi). FTIR and SEM analyzes clarify the characteristic bands of PVA, NaCMC and pyriproxyfen. The XRD and thermal analysis shows an increase in crystallinity due to pyriproxyfen (Xc:36.59%) and the active delivery alters the chain packing (T_g:74°C). The pyriproxyfen-based RRD developed, in addition to fulfilling the characteristics of prolonged release, allows it to be rolled up (compressed form) facilitating swallowing and subsequent conversion to an expanded form that is retained in the rumen throughout the treatment period.

Keywords: *intra-ruminal release, horn fly, polymeric films.*

How to cite: Alves, M. C. C., Oliveira, R. N., Oliveira, G. F., Ferreira, T. P., Middea, A., Tavares, M. I. B., Sabeça, H., Gomes, B. T., Rosado, L. H. G., Scott, F. B. & Cid, Y. P. (2024). Pyriproxyfen-based Rumino-Reticulum Device for horn fly control in cattle: development and characterization. *Polímeros: Ciência e Tecnologia*, 34(2), e20240019. <https://doi.org/10.1590/0104-1428.20230079>

1. Introduction

Polymers are commonly used to obtain controlled-release dosage systems, acting as drug reservoirs due to their polymeric properties^[1]. The United States Pharmacopeia (2022) defines controlled release as prolonging the release of the active substance (API) compared to that predicted for an immediate-release dosage form. Among its advantages are the reduction in the number of administrations and the increase in the average residence time in the gastrointestinal tract, improving the therapeutic effects^[2,3].

Polyvinyl alcohol (PVA) and carboxymethylcellulose (CMC) are biodegradable polymers with properties suitable for pharmaceutical uses, such as the ability to form films and prolonged drug release^[4,5]. PVA-NaCMC films are obtained by a crosslinking reaction. Therefore, their physicochemical properties are influenced by the chemical structure of the copolymer, such as the reduction of water permeability, favoring the development of controlled release systems^[5].

Haematobia irritans, or horn fly, is an obligate hematophagous parasite of cattle that generates painful bites that cause irritation and local stress in the dorsal region, resulting in deleterious effects on health, production, and performance of cattle^[5]. Brazilian livestock breeding stands out internationally with the largest bovine population in the world. The economic losses linked to this parasite explain why antiparasitics for ruminants represent the largest share of the animal health products market^[6,7]. *H. irritans* control is commonly carried out using chemical products, such as pyrethroids, organophosphates, phenyl pyrazoles and their various associations, by injectable, pour-on and spray formulations as well as impregnated earrings^[8].

Pyriproxyfen belongs to the insect growth regulation (IGR) class and is an alternative method to conventional pesticides. It is a juvenile hormone analog that regulates the growth and development of parasites in the immature stages, thus being more selective, less toxic and safer^[9-11]. It is indicated for use in controlling fleas and ticks in pets, and insects such as *Aedes aegypti*^[12,13]. Recently, its efficacy in controlling *H. irritans* administered intraruminal in multiple doses of immediate release was described^[10].

Developing controlled-release dosage forms for cattle aims to minimize the time and cost of treating the herd, focusing on animal welfare and long-term protection and reducing the management cost, particularly important aspects due to extensive livestock grazing in Brazil^[6,10]. Designing an Rumino-Reticulum Device (RRD) must take in consideration two important factors: the rumen environment conditions and the regurgitation reflexes. The unique anatomy and physiology of ruminants enable the long-term retention of devices in the rumen. However, to avoid regurgitation of RRDs, some strategies can be used, such as the use of particular geometrical shape that prevents regurgitation via the oesophagus. To reach such strategy, the device must present physical properties (breakage resistance and malleability) that allows it to be compressed in order to facilitate swallowed when administered and then convert to an expanded form that is retained for the duration of the treatment in rumen^[14]. In this context, this study aimed to develop and characterize a pyriproxyfen-based RRD consisting of films of poly(vinyl)alcohol (PVA) and sodium carboxymethylcellulose (NaCMC) for the control of *H. irritans* in cattle. The three-dimensional structures of the reticulated polymeric chains of films with controlled-release potential associated with oral efficacy of pyriproxyfen against *H. irritans* previously described^[10] support the work proposal.

2. Materials and Methods

2.1 Film preparation

The films were obtained by the solvent casting method based on Oliveira et al.^[15]. An aqueous PVA filmogenic solution (10% w/v) was obtained by mechanical stirring at 90 °C for 6 hours. NaCMC (2% w/v) was incorporated into the solution at room temperature under mechanical stirring for 30 minutes. Pyriproxyfen (0.00125% (w/v)) was solubilized in acetonitrile and added to the filmogenic solution. The final solution (5.0 mL) was degassed by ultrasound (Ultronique Q3.0/40), poured into silicone templates, and dried in an oven with constant air flow (Solab,

SL-102/1152), at 35 °C for 12 hours. The films were made measuring 144 cm² (18 cm x 8 cm) containing 226.40 mg of pyriproxyfen (1.5 mg/cm²). The drug content per film was calculated in order to reach the dose (mg/kg) with larvicidal efficacy against *H. irritans* described by Oliveira et al.^[10] The samples with and without the active ingredient were called PVA-NaCMC-P and PVA-NaCMC, respectively.

2.2 Physical-chemical characterization

The placebo (PVA-NaCMC) and film (PVA-NaCMC-P) samples were evaluated by physical-chemical tests of weight variation, surface pH, swelling degree, drug content, *in vitro* drug release, X-ray diffraction analysis (XRD), Fourier-transform infrared spectroscopy (FTIR), differential scanning calorimetry (DSC) and scanning electron microscopy (SEM). The film samples (PVA-NaCMC-P) after the *in vitro* release of the drug were also characterized by XRD, FTIR, DSC and SEM. The Figure 1 represents the chemical structure of pyriproxyfen.

2.3 Weight variation

The samples were randomly cut (1.0 cm²) from the film (n=3) and weighed individually and the results were expressed as mean ± SD. Assessments were performed in triplicate.

2.4 Surface pH

Samples with an average weight of 0.0224 g ± 0.01 were moistened in 5.0 mL of distilled water and the pH was measured on the surface of the film with a pH meter (PHS-3E Even). Analyses were performed in triplicate.

2.5 Swelling degree

The degree of swelling assay was adapted according to Oliveira et al. (2013)^[16]. Each sample (n=3, 1.0 cm²) was immersed in 5.0 mL of the artificial ruminal medium (ARM) solutions: Na₂HPO₄ (9.3g), NaHCO₃ (9.8g), NaCl (4.7g), KCl (5.7g), CaCl₂ (0.053g), MgCl₂ (0.128g), FeSO₂ (0.075g), MnSO₄ (0.004g), urea (0.07g) and qsp water (1000.0 mL), pH fixed at 6.9, for four h at 38 °C, with weighing at times of 0, 5, 10, 15, 20, 30, 45 minutes and 1, 2 and 4 hours. The swelling degree (SD) was calculated according to Equation 1, where W_s is the weight of the polymer after swelling and W_d is the weight of the polymer before swelling.

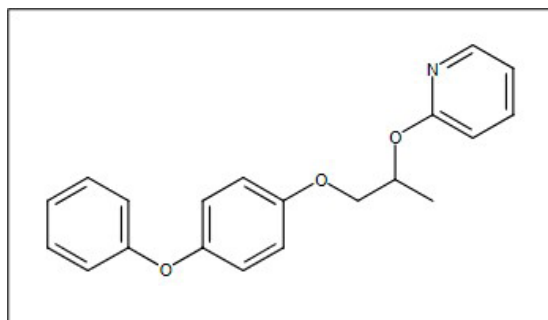


Figure 1. Chemical structure of Pyriproxyfen. CAS registry number: 95737-68-1. Molecular formula C₂₀H₁₉NO₃.

$$SD = 100 \left(\frac{WS - WD}{WD} \right) \quad (1)$$

2.6 Drug content

Samples (1 cm²) of the PVA-NaCMC-P film were diluted with 10.0 mL of acetonitrile and submitted to ultrasound for 2 hours. Drug content was measured by the LC-UV method under the following conditions. The chromatographic separation was performed using a C18 column (Kromasil, 3.5 μm; 4.6×100 mm; Tedia, Rio de Janeiro, Brazil), preceded by a C18 guard column (Kromasil, 3.5 μm; 4.6×10 mm; Tedia, Rio de Janeiro, Brazil), both maintained at 25 °C. The mobile phase consisted of acetonitrile: water (80:20, v/v) with a 1.5 mL/minute flow rate. The UV wavelength was 254 nm, and the injection volume was 10 μL. The experiment was performed in triplicate, and the average values were calculated.

2.7 In vitro drug release studies

Initially, the solubility studies were performed using a shake flask method at 38 °C and a pH range of 5.1 to 7.0^[17,18]. Samples were prepared with saturated solutions of pyriproxyfen in a medium of H₂O (pH 5.6), phosphate buffer (pH 6.5), and artificial ruminal medium (pH 6.9) in surfactant sodium dodecyl sulfate (SDS) concentrations of 1.0 and 5.0% p/v and absence, at 38 °C. The test was performed for 24 hours on a shaking platform (Shake Incubator, Cienlab), and the aliquots were centrifuged (CT 6000r, Cientec) at 3,000 rpm, 584,7 rcf (g) for 10 min. The supernatants were filtered through a membrane Durapore® Millex-HV (PVDF), (0.45 μm × 13 mm) and analyzed by LC-UV.

The *in vitro* drug release studies were performed at phosphate buffer medium (PB) pH 6.5, artificial ruminal medium (ARM) pH 6.9, and ruminal medium (RM) pH 6.9, at 39 °C under agitation (Shake Incubator, Cienlab) at 100 rpm. The ruminal medium (RM) was collected via an oral probe in cattle. It was diluted (1:10) in the artificial ruminal medium, packed in amber bottles with seals against CO₂ entry for medium maintenance. In each medium, film samples weighing 0.4767g ± 0.02 in the PB, 0.4708 ± 0.02g in the ARM, and 0.4869g ± 0.02 in the MR were immersed in 100 mL of the drug release medium. At time intervals of 1 to 60 days, 1 mL of the release medium was collected and the same amount of medium was replaced. The amount of released drug was analyzed by LC-UV, and the mechanism of release from the PVA-NaCMC-P samples was established by fitting the drug release kinetics data with applying three kinetic models: (1) zero-order: amount released per unit area (μg/cm²) versus time (h)(2) Higuchi: amount released per unit area (μg/cm²) versus the square root of time (h), and (3) first order: log of amount released per area (μg/cm²) versus time (h)^[19].

2.8 X rays diffraction analysis (XRD)

The samples placebo (PVA-NaCMC), film (PVA-NaCMC-P), Film_AM (film PVA-NaCMC-P post release at artificial medium) and Film_RM (film PVA-NaCMC-P post release at ruminal medium) were evaluated by X-ray diffraction analysis using a Bruker AXS D8 Advance Eco diffractometer (CETEM/UFRJ) with CuKα radiation at 40 kV

and 25 mA. The parameters used were angular diffraction range of 2θ = 5°-70°, step of 0.02° and step time of 2 s. The curves were smoothed by the Savitzky-Golay method, polynomial order 2, no boundary condition, 15 points per window, using the Origin-Pro Software. To calculate the samples' degree of crystallinity by XRD, Equation 2 was adapted^[18], where A_C is the crystalline area, and A_T is the total area under the curve. To obtain the crystalline area, deconvolution of each curve using Lorentz fitting with manual adjustment was performed (Origin-Pro Software).

$$X_c(\%) = 100 \frac{A_c}{A_T} \quad (2)$$

2.9 Fourier-transform infrared spectroscopy (FTIR)

Samples were evaluated for physical-chemical characterization by Fourier-transform infrared spectroscopy (FTIR) with a Bruker Vertex 70 spectrometer (USA), with wavenumber range of 400 cm⁻¹ to 4000 cm⁻¹ and 32 scans per sample. To plot the spectra, curves were smoothed (Savitzky-Golay method, 20 window points, polynomial order 2).

2.10 Differential scanning calorimetry (DSC)

The differential scanning calorimetry (DSC) analysis was performed with a TA Instruments Q-1000 calorimeter (IMA/UFRJ), with a heating rate of 10°C/min, temperature range of room temperature to 250 °C. The samples' T_g (glass transition temperature) and T_m (melting temperature) were obtained in the third cycle of heating (to avoid the samples' thermal history). The PVA's degree of crystallinity was calculated in the third cycle of heating according to Equation 3, where: w is the PVA weight fraction in the samples, ΔH_m (J/g) is the sample heat of fusion, and ΔH_m⁰ is the 100% crystalline PVA heat of fusion (161 J/g)^[19].

$$X_{cPVA} = 100 \frac{\Delta H_m}{w \Delta H_m^0} \quad (3)$$

2.11 Scanning electron microscopy (SEM)

The samples' morphology was evaluated with a Hitachi Tm 3030 Plus scanning electron microscope under high vacuum, at 15 kV, coated with gold (Bal-tec SCD 005 sputter coater) (CETEM/UFRJ).

2.12 Statistical analysis

Statistical differences between three or more groups were analyzed using the One-way analysis of variance (ANOVA) with Tukey's post hoc analysis. Statistical significance was set to a p value ≤ 0.05. Results are presented as mean ± standard deviation.

3. Results and Discussions

3.1 Weight variation, surface pH, and drug content

The weight variation evaluation demonstrated the homogeneity of the samples, with values of 0.0390 ± 0.01 and 0.0446 ± 0.02 g for the placebo (PVA-NaCMC) and formulation (PVA-NaCMC-P), respectively. The surface pH helped characterize

the films' acidic or basic indicators and did not vary between the PVA-NaCMC and PVA-NaCMC-P samples, obtaining values from 6.80 ± 0.02 to 6.50 ± 0.14 , indicating that the pH of the surface of the films is biocompatible with ruminal pH. The content value obtained for PVA-NaCMC-P was 104.81 ± 0.01 , in accordance with the acceptable range of 90.0 to 110.0% of the active agent in the formulation (Table 1).

3.2 Swelling degree

The swelling degree test evaluates the film's absorptive capacity, an important parameter to elucidate dissolution properties and release of the active by diffusion. The initial swelling degree was found to be 147.93% in 1 minute and increased over time, remaining stable at 60 minutes, with 331.40%, as shown in Figure 2.

The films consist of a crosslinked polymer network, with spaces between the polymer chains. Meshes allow the diffusion of liquids and small solutes, and one of the strategies for releasing actives trapped in polymeric films is controlled swelling^[20]. According to the results, the PVA-NaCMC-P film has fast absorptive capacity, stabilizing in 1 hour. To evaluate this profile and its influence on the active release, an *in vitro* release study was carried out.

3.3 Solubility study: shake flask

Pyriproxyfen's solubility ($\mu\text{g/mL}$) in the different dissolution media, with varying pH range (6.0 to 7.0), in the absence and presence of surfactant in various concentrations, is described in Table 2.

Pyriproxyfen undergoes hydrolysis in an acid medium, being more stable in buffers with pH ranging from 4.0 to 9.0^[21]. Since the bovine ruminal medium has a neutral pH (6.0 to 8.0), testing the solubility of pyriproxyfen under these conditions mimics the solubility and dissolution of the active agent under biological conditions^[18]. The phosphate

buffer dissolution media and the artificial ruminal medium showed no significant differences. The increase in solubility was directly related to the rise in SDS concentration in the basic media, with the 5.0% concentration having the highest solubility of the three media. The use of surfactants in dissolution media is one of the main strategies to increase the solubility of insoluble drugs such as pyriproxyfen, in addition, the ruminal medium has fatty acids that act as surfactants^[22]. Based on the results obtained, the value of the sink condition was 9.64 in ARM, being approximately nine times the total volume of the dissolution medium sufficient to prevent drug saturation and promote *in vitro* release.

3.4 In vitro drug release

The *in vitro* release profile of PVA-NaCMC-P films in the dissolution media phosphate buffer (PB), artificial ruminal medium (ARM), and ruminal medium (RM) is shown in Figure 3.

The dissolution profile of the PVA-NaCMC-P film in the PB, ARM, and MR media showed dissolved fractions from day 1, corresponding to 12.39%, 13.37%, and 11.18%, and on day 60 of 40.24%, 46.43%, and 49.39%, respectively.

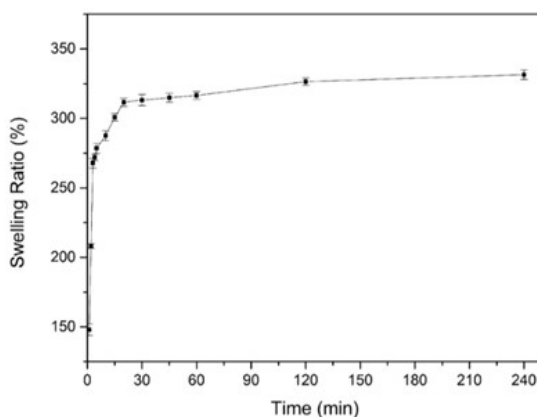


Figure 2. Swelling degree profile of PVA-NaCMC-P film in artificial ruminal medium (RAM).

Table 1. Results of Physicochemical evaluation of films. (n = 3).

Films	Weight Variation (g)*	Surface pH*	Assay (%)*
PVA-NaCMC	0.0390 ± 0.01	6.80 ± 0.02	-
PVA-NaCMC-P	0.0446 ± 0.02	6.50 ± 0.14	104.81 ± 0.01

*mean \pm dp.

Table 2. Solubility ($\mu\text{g/mL}$) of Pyriproxyfen obtained by shake flask assay.

Median	% SDS	Solubility ($\mu\text{g/mL}$)*
Water	-	4.95 ± 0.1^b
	1	414.31 ± 0.8^c
	5	2088.53 ± 1.5^d
Phosphate Buffer (PB)	-	0.39 ± 0.2^b
	1	398.86 ± 0.9^c
	5	2412.43 ± 0.8^d
Artificial Ruminal Median (ARM)	-	0.63 ± 0.2^b
	1	499.12 ± 0.9^c
	5	2349.02 ± 1.3^d

*Solubility \pm dp. Different letters differ significantly $P < 0.05$; Equal letters don't differ significantly. $P > 0.05$. Statistical analysis: One-Way ANOVA (Tukey).

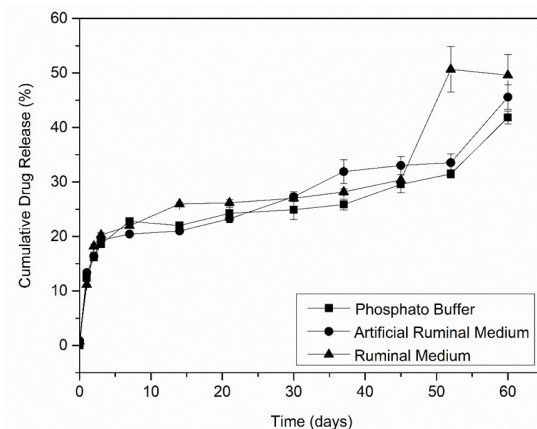


Figure 3. Drug release of PVA-NaCMC-P films determined in 100 mL of dissolution media (PB, ARM, RM) with SDS 5,0%; 100 rpm varying dissolution media.

Therefore, the one-way ANOVA and Tukey test indicated that the medium used did not significantly interfere with the release profile of the PVA-NaCMC-P formulation. Due to the support and control of the active release profile results together with the kinetics study, it can be stated that the formulation has the proper characteristics of a controlled release system.

3.5 In vitro release kinetics

The most linear portion (10 to 40 days) of each profile was chosen to determine the release kinetics for each formulation, and the three kinetic models were applied. The model that presented the highest linear correlation value was chosen as the kinetic model. The flux value (J) corresponds to the slope of the linear regression line. The flux (J) and linear correlation coefficient (r) values of the analyzed formulations are shown in Table 3.

In vitro release studies revealed pseudo-first-order kinetics (Higuchi), characterizing a diffusion-controlled release system. The dissolution media did not influence the kinetic profile. PVA-NaCMC hydrogels have been previously described for transporting drugs with sustained and controlled release, with several medical applications. Among its applications is the controlled release of drugs from transdermal dressings^[23], release of water-soluble drugs^[24], and release of orally administered peptides into the intestinal fluid^[25].

The films were analyzed after release to elucidate the influence of dissolution and the medium on the mechanical, thermal, and morphological characteristics. They were named film AM (sample loaded with pyriproxyfen after immersion in the artificial medium) and film RM (sample loaded with pyriproxyfen after immersion in the bovine rumen medium).

3.6 X-ray diffraction analysis (XRD)

The samples' XRD curves are displayed in Figure 4.

The increase of the crystallinity of the Film sample occurs due to the presence of pyriproxyfen, attributed to the high number of crystalline peaks in the sample. The presence of pyriproxyfen was observed by the diffraction peaks at $2\theta=13.93^\circ$ and 16.77° and the PVA peak's increased intensity at $2\theta=19.42^\circ$. The film_AM (PVA-NaCMC-P post release at artificial medium) sample presented a diffractogram similar to the Placebo sample, indicating pyriproxyfen release, although the film_RM (PVA-NaCMC-P post release at ruminal

medium) sample had increased intensity of pyriproxyfen peaks at $2\theta=13.91^\circ$ and $2\theta=16.62^\circ$, besides an extra peak at $2\theta=25.25^\circ$. To calculate the crystallinity degree of each sample by XRD, the PVA-NaCMC peaks at $2\theta=19.42^\circ$, $2\theta=22.68^\circ$ and $2\theta=40.53^\circ$ were considered crystalline ones, along with the pyriproxyfen peaks at $2\theta=13.93^\circ$ and 16.77° , a method adapted from^[26] (Figure 5).

Regarding the Placebo sample, it is composed of PVA and NaCMC. PVA presented a peak at $2\theta=19.42^\circ$, diffraction plane (101), a shoulder centered around $2\theta=22.68^\circ$, diffraction plane (200), as well as a broad peak at $2\theta=40.53^\circ$, a probable contribution of the PVA diffraction plane (110) or PVA diffraction plane (111)^[27]. Carboxymethyl cellulose might also have contributed to the peaks at $2\theta=19.42^\circ$ and $2\theta=22.68^\circ$

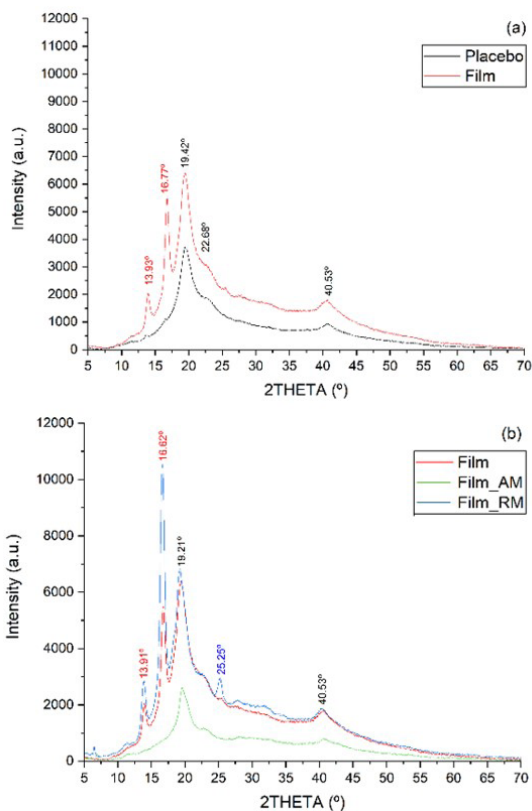


Figure 4. Diffractograms of (a) placebo and Film samples, (b) Film, Film_AM, and Film_RM samples.

Table 3. Determination of flux (J) and release kinetics (n=3) of PVA-NaCMC-P formulations in different dissolution media.

Dissolution median	Flux (J)*	Linear correlation coefficient (r)	Kinetics model
Phosphate Buffer	1.2525 ± 0.7	0.9831	Pseudo-first order
Artificial Ruminal Median	0.8434 ± 0.4	0.9089	
Ruminal Median	1.1836 ± 0.5	0.8571	
Phosphate Buffer	0.0658 ± 0.3	0.9511	Zero-order
Artificial Ruminal Median	0.0428 ± 0.6	0.8497	
Ruminal Median	0.0588 ± 0.5	0.7842	
Phosphate Buffer	0.0016 ± 0.2	0.9171	First-order
Artificial Ruminal Median	0.0010 ± 0.4	0.8286	
Ruminal Median	0.0015 ± 0.7	0.7109	

*Average values and their standard deviation.

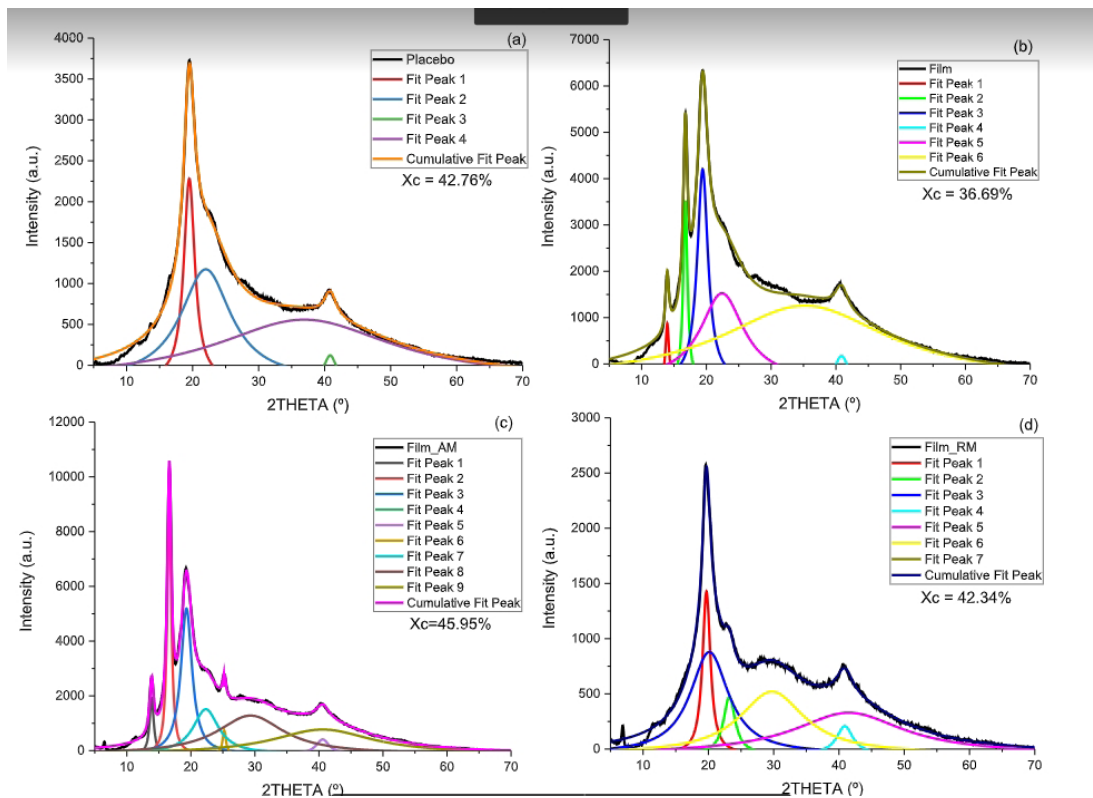


Figure 5. The deconvolution data, as well as the deconvoluted curves of the samples (a) placebo, (b) Film, (c) Film_AM, and (d) Film_RM.

since cellulose type I presents crystalline peaks at $2\theta=17^\circ$, 21° and 23° while cellulose type II presents diffraction peaks at $2\theta=20^\circ$ and 23° ^[28]. Na-CMC itself presents broad peaks in the region between $2\theta=10^\circ$ and $2\theta=20^\circ$, related to the diffraction planes (002) and (101)^[29].

The film sample had similar composition to the placebo sample, but pyriproxyfen was added, causing considerably more diffraction peaks, characteristic of some drugs^[30]. Pyriproxyfen presented diffraction peaks with high intensity in the range of $2\theta=17^\circ$ - 25° ^[31]. Despite the crystallinity of pyriproxyfen, its addition diminished the samples' degree of crystallinity. After immersion in artificial media, the film sample diffractogram was similar to the placebo one: the pyriproxyfen peaks were absent, indicating drug release. Nevertheless, after immersion in bovine rumen medium, the samples exhibited more intense pyriproxyfen peaks and an extra peak at $2\theta=25.25^\circ$. In addition, the sample crystallinity was higher after immersion in the artificial medium (probably due to the release of pyriproxyfen, leaving the polymer chains with more freedom to move and pack in crystallites^[15]). The Xc was similar to the placebo degree of crystallinity after immersion in bovine rumen medium.

3.7 Fourier-transform infrared spectroscopy (FTIR)

Compared to PVA and CMC, the Placebo sample (PVA-NaCMC) (Figure 6) presented similar bands to the original polymers. Still, some bands were displaced (indicated by arrows in Figure 6a), e.g., at 1647 and 1317 cm^{-1} . Among them, some were located between PVA and CMC bands (indicated by arrows and lines in Figure 6a, i.e., 3268 , 1145 , 1083 cm^{-1}),

probably indicating miscibility between polymers^[31], and physical interaction between PVA and CMC^[32]. In addition, a band related to crystalline cellulose I, at 896 cm^{-1} , was detected^[33]. The samples loaded with pyriproxyfen (named "Film") presented not only some shifted bands, but low intensity bands probably related to pyriproxyfen, e.g., at 2958 cm^{-1} , due to C-H (stretching/vibration/deformation) from the aromatic ring^[34]; 1708 cm^{-1} , attributed to $\text{C}=\text{O}$ ^[35]; 1658 cm^{-1} , related to $(\text{C}=\text{O})$ coupled with $\nu(\text{CN})$, ($\text{CCN})$ ^[36] (indicated by arrows in Figure 6b). The membrane evaluated after immersion in artificial medium did not have new bands. Although slight band displacement was observed, the absence of many NaCMC bands might be related to the high hydrophilicity of NaCMC^[37]. The media might leach out amorphous NaCMC chains, resulting in absent bands^[32]. The identified effect agrees with the results of the XRD and DSC analysis, where the dissolution of NaCMC in the media led to more freedom of movement of PVA chains, resulting in crystallization^[38]. The same effect was encountered in samples immersed in rumen medium, but a band at 1558 cm^{-1} was identified (indicated by an arrow in Figure 6 d). It might have been related to amide II vibrations of proteins ($\nu(\text{C}=\text{O})$ and $\nu(\text{C}-\text{N})$ of the peptide backbone), presented in the rumen medium^[39].

3.8 Differential scanning calorimetry (DSC)

The placebo (PVA-NaCMC), film (PVA-NaCMC-P), and film_RM (PVA-NaCMC-P post release at ruminal medium) samples presented approximately similar Tg values (temperature in which the amorphous chains present

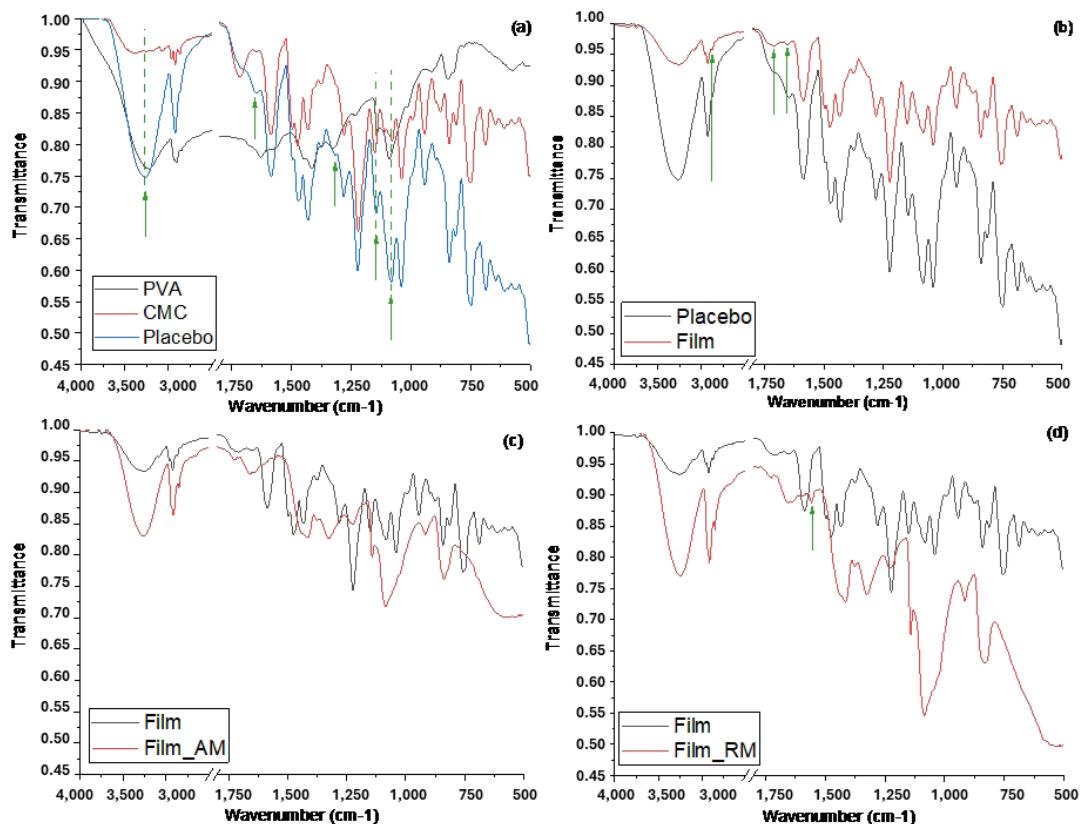


Figure 6. FTIR diffractograms of each sample .

mobility^[40], while film_AM had higher Tg than the other samples (Figure 7).

The high Tg of this sample might be related to the pyriproxyfen delivery, since the amorphous polymer chains might have rearranged themselves in the near absence of the drug. The Tm and Xc values diminished with a similar trend: Placebo > Film > Film_AM. The melting temperature is related to the melting of the hydrogels' crystallites, which decreases as the crystallite imperfections increase^[41]. Probably pyriproxyfen interferes with the crystallites' formation and the swelling in the artificial media. The degree of crystallinity is related to the chains' organization in the hydrogel^[42]. It followed the same trend as Tm, where pyriproxyfen and the artificial media interfered with the polymers' chain organization according to the XRD results. After immersion in bovine rumen medium, there was an increase in both Xc and Tm, indicating that the hydrogel-medium interactions promote chain organization for formation of crystallites.

3.9 Scanning electron microscopy (SEM)

The porosity of the film sample was greater than that of the placebo one (Figure 8). The addition of pyriproxyfen altered the samples' porosity distribution. After inclusion of artificial media, there were crystals (needle-like particles) on the fracture surface, indicating the probable presence of nanometric crystals related to the artificial media. The fracture surface of film_RM was similar to that of the placebo.

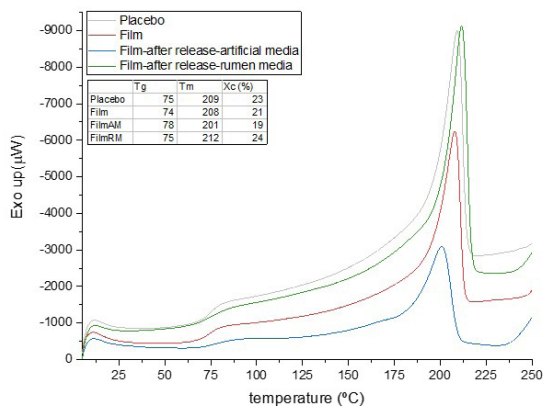


Figure 7. DSC curves of each sample.

After immersion in both media, the samples presented low porosity, possibly indicating changes in the matrix due to drug delivery and polymer chain rearrangement promoted by the immersion in media^[43].

Pyriproxyfen was encountered in the samples diffractograms, while the same technique indicated the drug release in the artificial medium and drug persistence after immersion in bovine rumen medium. The thermal analysis revealed that pyriproxyfen, as well as its delivery, altered the chain packing. In addition, the FTIR analysis showed

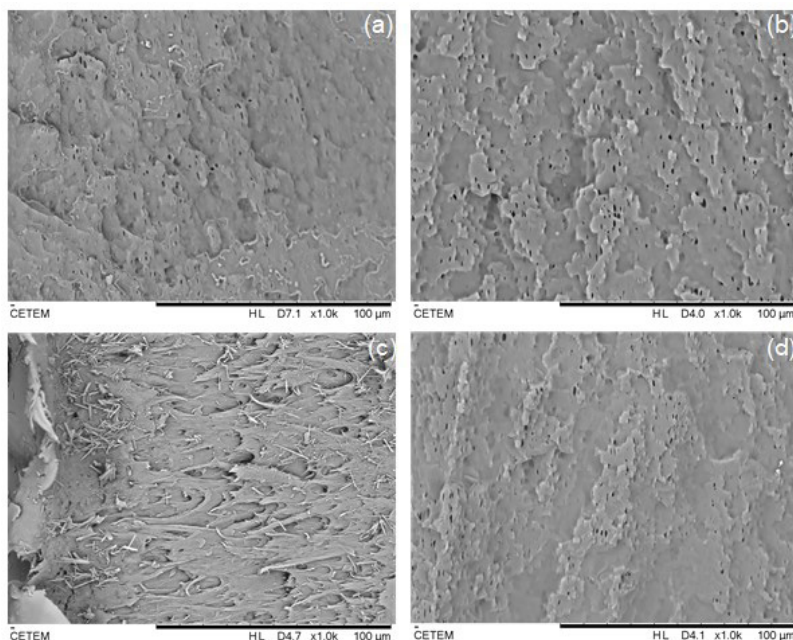


Figure 8. SEM images of the fracture surface of (a) placebo, (b) Film, (c) Film_AM, and (d) Film_RM samples.

that PVA with low NaCMC was probably the remaining material after immersion in the media. The porosity of the films diminished after immersion, which might have been related to drug delivery and NaCMC dissolution.

As previously reported, pyriproxyfen when administered by the intra-ruminal route in cattle does not undergo degradation in the ruminal environment being eliminated in its active form in feces with strong IGD activity against *H. irritans*^[10]. The pyriproxyfen-based RRD consisting of films of poly(vinyl)alcohol (PVA) and sodium carboxymethylcellulose (NaCMC) developed in this work, in addition to full fill the characteristics of prolonged release, allows it to be wound (compressed form) resisting breakage or cracking and convert to an expanded form that is retained for the duration of the treatment. However, in order to verify the feasibility and biocompatibility of the device for oral administration in cattle, *in vivo* studies are necessary to identify potential advantages and disadvantages of oral application to ensure animal health and safety.

In the Brazilian livestock market, technological innovation is necessary to promote animal health and well-being and offer practicality and safety in veterinary therapy. The success of these controlled release systems (RDD) is related to the physicochemical characteristics of the polymer, guaranteeing advantages such as reduced animal stress, reduced handling risks and medication administration. The current market has delivery systems in the form of injectable solutions, impregnated earrings and pour-on solutions, therefore, the development of this device allows the market to resume with innovative oral applications.

4. Conclusion

The PVA-NaCMC-Pyriproxyfen film presented homogeneity in the weight variation test, along with content and pH

parameters satisfactory for the purpose. PVA, NaCMC and pyriproxyfen were identified in the FTIR spectra. SEM images showed changes in the porosity distribution after the addition of pyriproxyfen. XRD analysis showed an increase in crystallinity due to the presence of pyriproxyfen. In addition, DSC analysis revealed that pyriproxyfen and its delivery altered chain packing. Furthermore, the release study corroborated the pseudo-first-order kinetics model, characterizing a controlled drug release system without the influence of the dissolution medium (PB, ARM, RM). The pyriproxyfen-based RRD consisting of films of poly(vinyl)alcohol (PVA) and sodium carboxymethylcellulose (NaCMC) developed, in addition to fulfilling the characteristics of prolonged release, allows it to be rolled up (compressed form) facilitating swallowing and subsequent conversion to an expanded form that is retained in the rumen throughout the treatment period, presenting potential for application in the control of horn flies in cattle.

5. Author's Contribution

- **Conceptualization** – Melina Cardilo Campos Alves; Luiz Henrique Guerreiro Rosado; Yara Peluso Cid.
- **Data curation** – Renata Nunes Oliveira; Thais Paes Ferreira.
- **Formal analysis** – Antonieta Middea; Maria Inês Bruno Tavares.
- **Funding acquisition** – Yara Peluso Cid; Fábio Barbour Scott.
- **Investigation** – Melina Cardilo Campos Alves.
- **Methodology** – Melina Cardilo Campos Alves; Gabriela Ferreira de Oliveira; Bruno de Toledo Gomes; Hugo Sabeça.
- **Project administration** – Yara Peluso Cid.
- **Resources** – Fábio Barbour Scott; Yara Peluso Cid.

- **Software** – NA.
- **Supervision** – Yara Peluso Cid; Renata Nunes de Oliveira.
- **Validation** – NA.
- **Visualization** – Melina Cardilo Campos Alves; Yara Peluso Cid.
- **Writing – original draft** – Melina Cardilo Campos Alves.
- **Writing – review & editing** – Melina Cardilo Campos Alves; Yara Peluso Cid; Renata Nunes de Oliveira.

6. Acknowledgements

This work was carried out with the support of CAPES and FAPERJ Process SEI E-26/201.381/2021 (260532). To the Analytical Center of QI and CETEM-UFRJ for the partnership and analyzes made.

7. References

1. Tran, T. T. D., & Tran, P. H. L. (2019). Controlled release film forming systems in drug delivery: the potential for efficient drug delivery. *Pharmaceutics*, *11*(6), 290. <http://doi.org/10.3390/pharmaceutics11060290>. PMID:31226748.
2. United States Pharmacopeia. (2022, November). *43 - National Formulary 38 (USP 43 - NF 38)*. Rockville: United States Pharmacopeia.
3. Adepui, S., & Ramakrishna, S. (2021). Controlled drug delivery systems: current status and future directions. *Molecules (Basel, Switzerland)*, *26*(19), 5905. <http://doi.org/10.3390/molecules26195905>. PMID:34641447.
4. Kim, M. N., & Yoon, M. G. (2010). Isolation of strains degrading poly(Vinyl alcohol) at high temperatures and their biodegradation ability. *Polymer Degradation & Stability*, *95*(1), 89-93. <http://doi.org/10.1016/j.polymdegradstab.2009.09.014>.
5. Khoramabadi, H. N., Arefian, M., Hojjati, M., Tajzad, I., Mokhtarzade, A., Mazhar, M., & Jamavari, A. (2020). A review of polyvinyl alcohol/carboxymethyl cellulose (PVA/CMC) composites for various applications. *Journal of Composites and Compounds*, *2*(3), 69-76. <http://doi.org/10.29252/jcc.2.2.2>.
6. Grisi, L., Leite, R. C., Martins, J. R. S., Barros, A. T. M., Andreotti, R., Caçado, P. H. D., Leon, A. A. P., Pereira, J. B., & Villela, H. S. (2014). Reassessment of the potential economic impact of cattle parasites in Brazil. *Revista Brasileira de Parasitologia Veterinária*, *23*(2), 150-156. <http://doi.org/10.1590/S1984-29612014042>. PMID:25054492.
7. Sindicato Nacional da Indústria de Produtos para Saúde Animal - SINDAN. (2022, November 11). Retrieved in 2023, October 3, from https://sindan.org.br/wp-content/uploads/2023/10/Fechamento-Mercado-2022_div-1.pdf
8. Taylor, M. A. (2001). Recent developments in ectoparasiticides. *Veterinary Journal (London, England)*, *161*(3), 253-268. <http://doi.org/10.1053/tvj.2000.0549>. PMID:11352483.
9. Faria, A. B. C. (2009). Revisão sobre alguns grupos de inseticidas utilizados no manejo integrado de pragas florestais. *Ambiência - Revista do Setor de Ciências Agrárias e Ambientais*, *5*(2), 345-358. Retrieved in 2023, October 3, from <https://revistas.unicentro.br/index.php/ambiencia/article/view/347/pdf>
10. Oliveira, G. F., Magalhães, V. S., Alves, M. C. C., Jesus, I. L. R., Medeiros, M. T., Gomes, B. T., Calado, S. B., Melo, R. C., Cid, Y. P., & Scott, F. B. (2021). Evaluation of pyriproxyfen in cattle by oral treatment: an alternative to control Haematobia irritans. *Veterinary Parasitology*, *299*, 109565. <http://doi.org/10.1016/j.vetpar.2021.109565>. PMID:34507202.
11. Apolinário, R., & Feder, D. (2021). Existing potentials in Insect Growth Regulators (IGR) for crop pest control. *Research, Social Development*, *10*(1), e35910111726. <http://doi.org/10.33448/rsd-v10i1.11726>.
12. Albuquerque, M. F. P. M., Souza, W. V., Mendes, A. C. G., Lyra, T. M., Xiemenes, R. A. A., Araújo, T. V. B., Braga, C., Miranda-Filho, D. B., Martelli, C. M. T., & Rodrigues, L. C. (2016). Pyriproxyfen and the microcephaly epidemic in Brazil - an ecological approach to explore the hypothesis of their association. *Memórias do Instituto Oswaldo Cruz*, *111*(12), 774-776. <http://doi.org/10.1590/0074-02760160291>. PMID:27812601.
13. Vythilingam, I., Luz, B. M., Hanni, R., Beng, T. S., & Huat, T. C. (2005). Laboratory and field evaluation of the insect growth regulator pyriproxyfen (Sumilarv 0.5 G) against dengue vectors. *Journal of the American Mosquito Control Association*, *21*(3), 296-300. [http://doi.org/10.2987/8756-971X\(2005\)21\[296:LA FEOT\]2.0.CO;2](http://doi.org/10.2987/8756-971X(2005)21[296:LA FEOT]2.0.CO;2). PMID:16252520.
14. Vandamme, T. F., & Ellis, K. J. (2004). Issues and challenges in developing ruminal drug delivery systems. *Advanced Drug Delivery Reviews*, *56*(10), 1415-1436. <http://doi.org/10.1016/j.addr.2004.02.011>. PMID:15191790.
15. Oliveira, R. N., McGuinness, G. B., Rouze, R., Quilty, B., Cahill, P., Soares, G. D. A., & Thiré, R. M. S. M. (2015). PVA hydrogels loaded with a Brazilian propolis for burn wound healing applications. *Journal of Applied Polymer Science*, *132*(25), 1-12. <http://doi.org/10.1002/app.42129>.
16. Oliveira, R. N., Rouzé, R., Quilty, B., Alvez, G. G., Soares, G. D. A., Thiré, R. M. S. M., & McGuinness, G. B. (2013). Mechanical properties and in vitro characterization of polyvinyl alcohol-nano-silver hydrogel wound dressings. *Interface Focus*, *4*(1), 120130049. <http://doi.org/10.1098/rsfs.2013.0049>. PMID:24501677.
17. Agência Nacional de Vigilância Sanitária - ANVISA. (2013, June 17). *Nota Técnica 003/2013*. Brasília: Agência Nacional de Vigilância Sanitária.
18. Apley, M., Crist, B., Gonzalez, M. A., Hunter, R. P., Martinez, M. N., Modric, S., Papich, M. G., Parr, A. F., Riviere, J. E., & Marques, M. R. C. (2013). Solubility criteria for veterinary drugs-workshop report. *Dissolution Technologies*, *39*(4), 22-35. <http://doi.org/10.14227/DT240117P22>.
19. Chou, C.-T., Shi, S.-C., & Chen, C.-K. (2021). Sandwich-Structured, Hydrophobic, Nanocellulose-Reinforced Polyvinyl Alcohol as an Alternative Straw Material. *Polymers*, *13*(24), 4447. <http://doi.org/10.3390/polym13244447>. PMID:34960998.
20. Li, J., & Mooney, D. J. (2016). Designing hydrogels for controlled drug delivery. *Nature Reviews. Materials*, *1*(12), 16071. <http://doi.org/10.1038/natrevmats.2016.71>. PMID:29657852.
21. Tassone, S., Fortina, R., & Peiretti, P. G. (2020). In vitro techniques using the daisy incubator for the assessment of digestibility: a review. *Animals (Basel)*, *10*(5), 775. <http://doi.org/10.3390/ani10050775>. PMID:32365689.
22. Oliveira, R. N., Moreira, A. P. D., Thiré, R. M. S. M., Quilty, B., Passos, T. M., Simon, P., Mancini, M. C., & McGuinness, G. B. (2017). Absorbent polyvinyl alcohol-sodium carboxymethyl cellulose hydrogels for propolis delivery in wound healing applications. *Polymer Engineering and Science*, *57*(11), 1224-1233. <http://doi.org/10.1002/pen.24500>.
23. Agarwal, R., Alam, M. S., & Gupta, B. (2013). Polyvinyl alcohol-polyethylene oxide-carboxymethyl cellulose membranes for drug delivery. *Journal of Applied Polymer Science*, *129*(6), 3728-1836. <http://doi.org/10.1002/app.39144>.
24. Ye, J., Liu, L., Lan, W., & Xiong, J. (2023). Targeted release of soybean peptide from CMC/PVA hydrogels in simulated intestinal

- fluid and their pharmacokinetics. *Carbohydrate Polymers*, 310, 120713. <http://doi.org/10.1016/j.carbpol.2023.120713>. PMID:36925260.
25. Schoeler, M. N., Scremin, F. R., Mendonça, N. F., Benetti, V. P., Jesus, J. A., Basso, R. L. O., & Bittencourt, P. R. S. (2020). Cellulose nanofibers from cassava agro-industrial waste as reinforcement in Pva films. *Química Nova*, 43(6), 711-717. <http://doi.org/10.21577/0100-4042.20170542>.
26. Tang, C.-M., Tian, Y.-H., & Hsu, S.-H. (2015). Poly(vinyl alcohol) nanocomposites reinforced with bamboo charcoal nanoparticles: mineralization behavior and characterization. *Materials (Basel)*, 8(8), 4895-4911. <http://doi.org/10.3390/ma8084895>. PMID:28793480.
27. Machado, G. O. (2000). *Preparação e caracterização de CMC e CMC graftizada* (Master's thesis). Universidade de São Paulo, São Carlos. <http://doi.org/10.11606/D.88.2000.tde-11092001-160555>.
28. Sunardi, S., Febriani, N. M., & Junaidi, A. B. (2017). Preparation of carboxymethyl cellulose produced from purun tikus (*Eleocharis dulcis*). *IOP Conference Series. Materials Science and Engineering*, 1868, 020008. <http://doi.org/10.1063/1.4995094>.
29. Cardoso, V. M. O., Cury, B. S. F., Evangelista, R. C., & Gremião, M. P. D. (2017). Development and characterization of cross-linked gellan gum and retrograded starch blend hydrogels for drug delivery applications. *Journal of the Mechanical Behavior of Biomedical Materials*, 65, 317-333. <http://doi.org/10.1016/j.jmbbm.2016.08.005>. PMID:27631170.
30. Gurarlan, A., Shen, J., Caydamli, Y., & Tonelli, A. E. (2015). Pyriproxyfen cyclodextrin inclusion compounds. *Journal of Inclusion Phenomena and Macrocyclic Chemistry*, 82(3), 489-496. <http://doi.org/10.1007/s10847-015-0526-7>.
31. Reddy, R., Okigbo, R. N., & Putheti, M. (2016). Correlation of the miscibility of commercially important polymers PVC/PMMA and PS/PMMA in dilute solutions and in solid state. *Science Advances and Engineering Research*, 2(2), 11-15. Retrieved in 2023, October 3, from <https://www.primescholarslibrary.org/articles/correlation-of-the-miscibility-of-commercially-important-polymers-pvcpmma-and-pspmma-in-dilute-solutions-and-in-solid-st.pdf>
32. Santos, G. S., Santos, N. R. R., Pereira, I. C. S., Andrade Júnior, A. J., Lima, E. M. B., Minguita, A. P., Rosado, L. H. G., Moreira, A. P. D., Middea, A., Prudencio, E. R., Luchese, R. H., & Oliveira, R. N. (2020). Layered cryogels laden with Brazilian honey intended for wound care. *Polímeros: Ciência e Tecnologia*, 30(3), e2020031. <http://doi.org/10.1590/0104-1428.06820>.
33. Yang, Y. P., Zhang, Y., Lang, Y. X., & Yu, M. H. (2017). Structural ATR-IR analysis of cellulose fibers prepared from a NaOH complex aqueous solution. *IOP Conference Series. Materials Science and Engineering*, 213(1), 012039. <http://doi.org/10.1088/1757-899X/213/1/012039>.
34. Alves, M. C. C. (2021, July 19-22). *Poly(vinyl)alcohol-based films containing pyriproxyfen against Haematobia irritans in cattle: formulation development, physico-chemical characterization and in vitro drug release*. In *Proceedings of the 28th Conference of the World Association for the Advancement of Veterinary Parasitology WAAVP 2021* (pp. 492). Dublin, Ireland.
35. Yang, K. W., Murphy, D. L., White, C. S., Parfenova, M. N., McDaniel, J. D., & Ko, J. (2006). *U.S. Patent No US8226963B2*. Washington, DC: U.S. Patent and Trademark Office. Retrieved in 2023, October 3, from <https://patents.google.com/patent/US8226963B2/en>
36. Alromeed, A. A., Scrano, L. A., Bufo, S. A., & Undabeytia, T. (2015). Slow-release formulations of the herbicide MCPA by using clay-protein composites. *Pest Management Science*, 71(9), 1303-1310. <http://doi.org/10.1002/ps.3929>. PMID:25346289.
37. Rahman, S., Hasan, S., Nitai, A. S., Nam, S., Karmakar, A. K., Ahsan, S., Shiddiky, M. J. A., & Ahmed, M. B. (2021). Recent developments of carboxymethyl cellulose. *Polymers (Basel)*, 13(8), 1345. <http://doi.org/10.3390/polym13081345>. PMID:33924089.
38. Zuo, Z., Zhang, Y., Zhou, L., Liu, Z., Jiang, Z., Liu, Y., & Tang, L. (2021). Mechanical behaviors and probabilistic multiphase network model of polyvinyl alcohol hydrogel after being immersed in sodium hydroxide solution. *RSC Advances*, 11(19), 11468-11480. <http://doi.org/10.1039/D1RA00653C>. PMID:35423654.
39. Liu, D., Wu, P., & Jiao, P. (2016). Researching rumen degradation behaviour of protein by FTIR spectroscopy. *Czech Journal of Animal Science*, 60(1), 25-32. <http://doi.org/10.17221/7908-CJAS>.
40. Iijima, M., Kosaka, S., Hatakeyama, T., & Hatakeyama, H. (2016). Phase transition of poly(vinyl alcohol) hydrogel filled with micro-fibrillated cellulose. *Journal of Thermal Analysis and Calorimetry*, 123(3), 1809-1815. <http://doi.org/10.1007/s10973-015-4725-7>.
41. Fakirov, S., Cagiao, M. E., Baltá-Calleja, F. J., Sapundjieva, D., & Vassileva, E. D. (1999). Melting of gelatin crystals below glass transition temperature: a direct crystal-glass transition as revealed by microhardness. *International Journal of Polymeric Materials*, 43(3-4), 195-206. <http://doi.org/10.1080/00914039908009685>.
42. Bustamante-Torres, M., Romero-Fierro, D., Arcentales-Vera, B., Palomino, K., Magaña, H., & Bucio, E. (2021). Hydrogels classification according to the physical or chemical interactions and as stimuli-sensitive materials. *Gels (Basel, Switzerland)*, 7(4), 182. <http://doi.org/10.3390/gels7040182>. PMID:34842654.
43. Zhang, M., Bhattarai, N., & Matsen, F. A. (2014). *US Patent No US8663686B2*. Washington, DC: U.S. Patent and Trademark Office. Retrieved in 2023, October 3, from <https://patents.google.com/patent/US8663686B2/en>

Received: Oct. 03, 2023

Revised: Apr. 15, 2024

Accepted: Apr. 23, 2024